# Propagating director bend fluctuations in nematic liquid crystals

Anja Humpert[1,*] and Michael P. Allen[1,2,†]

[1] *Department of Physics, University of Warwick,*
*Coventry CV4 7AL, United Kingdom*
[2] *H. H. Wills Physics Laboratory, Royal Fort,*
*Tyndall Avenue, Bristol BS8 1TL, United Kingdom*

(Dated: December 17, 2014)

## Abstract

We show, by molecular simulation, that for a range of standard, coarse-grained, nematic liquid crystal models, the director bend fluctuation is a propagating mode. This is in contrast to the generally-accepted picture of nematic hydrodynamics, in which all the director modes (splay, twist, bend, and combinations thereof) are overdamped. By considering the various physical parameters that enter the equations of nematodynamics, we propose an explanation of this effect, and conclude that propagating bend fluctuations may be observable in some experimental systems.

PACS numbers: 83.10.Rs, 83.80.Xz, 47.11.Mn, 47.57.Lj

Most of the interesting properties of nematic liquid crystals [1–3] are determined by the Frank elastic constants $K_1$, $K_2$ and $K_3$ appearing in the static continuum theory [4–6], and the various Leslie coefficients $\alpha_1 \dots \alpha_6$ (viscosities) which enter the equations of nematodynamics [7–11]. The orientational relaxation of the space- and time-dependent nematic director $\mathbf{n}(\mathbf{r}, t)$, and its coupling to the hydrodynamic velocity field $\mathbf{v}(\mathbf{r}, t)$, may be accessed experimentally at low wavenumber $k$ and frequency $\omega$ by dynamic light scattering. Ever since the first analysis of such experiments, it has been argued on the basis of the relative orders of magnitudes of the elastic and viscosity coefficients [12, 13], that these modes decay exponentially, rather than oscillating in time. For example, the review of Stephen and Straley [13] states: "The orientation fluctuations of the director are coupled to the fluid velocity by viscous effects, and in fact are overdamped: the modes which the elastic theory ... predicts do not propagate". Similar statements appear in the textbook derivations [1, 2] and this view has been supported by experiment over subsequent years [14–17].

Particle-based molecular simulations allow us to connect the values of the coefficients of orientational elasticity and viscosity to molecular structure and interactions, and verify the assumptions of the continuum theory. We have recently conducted molecular dynamics simulations, using several variants of the Gay-Berne potential [18], a well-established coarse-grained model of mesogens. In order to reliably establish the limiting low-$(k, \omega)$ behaviour, and distinguish it from effects occurring at the molecular scale, we employed system sizes significantly larger than previous studies of elastic phenomena. By measuring equilibrium thermal director fluctuations as a function of wave-vector, we obtained accurate estimates of the Frank elastic constants $K_1 - K_3$. Full details will be given in a separate publication [19], but the techniques are quite standard [20–22]. We also calculated the equilibrium time correlation functions of pure splay, twist and bend director fluctuations at low $k$. Once more, full details will be given separately [19], but since these are our key results, we give a brief account here.

In a Cartesian coordinate system $(\mathbf{e}_1, \mathbf{e}_2, \mathbf{e}_3)$, we define $\mathbf{e}_3$ to lie along the equilibrium director $\mathbf{n}$ [12, 13]; fluctuations of the director are then written $\delta\mathbf{n} = (\delta n_1, \delta n_2, 0)$. The wave-vector $\mathbf{k} = (k_1, 0, k_3)$ is taken to lie in the $\mathbf{e}_1$–$\mathbf{e}_3$ plane. Denoting spatial Fourier components by $\delta\tilde{\mathbf{n}}(\mathbf{k},t)$, where $t$ is the time, we define

$$c_i(\mathbf{k},t) = \big\langle \delta\tilde{n}_i(\mathbf{k},t)\delta\tilde{n}_i(-\mathbf{k},0)\big\rangle / \big\langle \big|\delta\tilde{n}_i(\mathbf{k})\big|^2 \big\rangle \,, \quad i = 1, 2,$$

and the time correlation functions of interest are

$$c_{\text{splay}}(k,t) = c_1(k\mathbf{e}_1,t) \ , \quad c_{\text{twist}}(k,t) = c_2(k\mathbf{e}_1,t) \ ,$$
$$c_{\text{bend}}(k,t) = c_1(k\mathbf{e}_3,t) = c_2(k\mathbf{e}_3,t) \ .$$

The Gay-Berne potential [18, 23, 24] describes the interaction between roughly ellipsoidal particles, and is widely used to simulate liquid crystals. For a pair of identical uniaxial particles $i$, $j$, it has a shifted, Lennard-Jones form

$$U(\mathbf{u}_i,\mathbf{u}_j,\mathbf{r}_{ij}) = 4\epsilon_{ij}\left[\varrho_{ij}^{-12} - \varrho_{ij}^{-6}\right] \,,$$

and it depends on the orientation (unit) vectors $\mathbf{u}_i$, $\mathbf{u}_j$, and the center-center separation vector $\mathbf{r}_{ij} = \mathbf{r}_i - \mathbf{r}_j$, as follows:

$$\varrho_{ij} = \varrho(\mathbf{u}_i,\mathbf{u}_j,\hat{\mathbf{r}}_{ij}) = \frac{r_{ij} - \sigma(\mathbf{u}_i,\mathbf{u}_j,\hat{\mathbf{r}}_{ij}) + \sigma_0}{\sigma_0} \,,$$
$$\epsilon_{ij} = \epsilon(\mathbf{u}_i,\mathbf{u}_j,\hat{\mathbf{r}}_{ij}) = \epsilon_0\, \epsilon_1^{\nu}(\mathbf{u}_i,\mathbf{u}_j)\, \epsilon_2^{\mu}(\mathbf{u}_i,\mathbf{u}_j,\hat{\mathbf{r}}_{ij}) \,.$$

Here $\hat{\mathbf{r}}_{ij} = \mathbf{r}_{ij}/r_{ij}$ and $r_{ij} = |\mathbf{r}_{ij}|$. The parameter $\sigma_0$ represents the width of the particle, while $\epsilon_0$ determines the overall strength of the potential; units of length and energy are chosen such that $\sigma_0 = 1$ and $\epsilon_0 = 1$. The range function $\sigma(\mathbf{u}_i,\mathbf{u}_j,\hat{\mathbf{r}}_{ij})$ and energy functions $\epsilon_1(\mathbf{u}_i,\mathbf{u}_j)$, $\epsilon_2(\mathbf{u}_i,\mathbf{u}_j,\hat{\mathbf{r}}_{ij})$, depend on relative orientations:

$$\sigma(\mathbf{u}_i,\mathbf{u}_j,\hat{\mathbf{r}}_{ij}) = \sigma_0 \left[1 - \frac{\chi}{2}\left(\frac{(\hat{\mathbf{r}}_{ij}\cdot\mathbf{u}_i + \hat{\mathbf{r}}_{ij}\cdot\mathbf{u}_j)^2}{1+\chi\mathbf{u}_i\cdot\mathbf{u}_j} + \frac{(\hat{\mathbf{r}}_{ij}\cdot\mathbf{u}_i - \hat{\mathbf{r}}_{ij}\cdot\mathbf{u}_j)^2}{1-\chi\mathbf{u}_i\cdot\mathbf{u}_j}\right)\right]^{-1/2} \,,$$
$$\epsilon_1(\mathbf{u}_i,\mathbf{u}_j) = \left[1 - \chi^2(\mathbf{u}_i\cdot\mathbf{u}_j)^2)\right]^{-1/2} \,,$$
$$\epsilon_2(\mathbf{u}_i,\mathbf{u}_j,\hat{\mathbf{r}}_{ij}) = 1 - \frac{\chi'}{2}\left[\frac{(\hat{\mathbf{r}}_{ij}\cdot\mathbf{u}_i + \hat{\mathbf{r}}_{ij}\cdot\mathbf{u}_j)^2}{1+\chi'\mathbf{u}_i\cdot\mathbf{u}_j} + \frac{(\hat{\mathbf{r}}_{ij}\cdot\mathbf{u}_i - \hat{\mathbf{r}}_{ij}\cdot\mathbf{u}_j)^2}{1-\chi'\mathbf{u}_i\cdot\mathbf{u}_j}\right] \,.$$

Here

$$\chi = \frac{\kappa^2 - 1}{\kappa^2 + 1} \,, \qquad \chi' = \frac{\kappa'^{1/\mu} - 1}{\kappa'^{1/\mu} + 1}$$

where $\kappa$ is the length-to-width ratio of the particle and $\kappa'$ is the ratio of well depths for the side-to-side and end-to-end configurations of two molecules. $\nu$ and $\mu$ are two adjustable exponents which allow considerable flexibility in defining a family of Gay-Berne potentials. Different versions of the potential are identified by the GB$(\kappa, \kappa', \mu, \nu)$ notation of Bates and Luckhurst [25].

We have simulated GB$(3.0, 5.0, 2, 1)$, the original suggestion of Gay and Berne [18], for which the phase diagram has been well studied [26], and GB$(3.0, 5.0, 1, 3)$, proposed by Berardi *et al.* [23], which has the advantage of a wider nematic range. For all simulations the cutoff for the interactions was chosen to be $5\sigma_0$. $N = 512\,000$ particles were used, in cubic periodic boundaries, giving simulation box lengths $L > 100\sigma_0$. The particle mass $m_0$ is taken to be unity, leading to a basic unit of time $\tau_0 = \sigma_0\sqrt{m_0/\epsilon_0}$. All results reported here are referred to these units. The moment of inertia corresponded to uniform mass distribution within the ellipsoidal particle. Each system was equilibrated for $4 \times 10^5$ steps, followed by a production run of $1.9 \times 10^6$ steps, with a timestep $\Delta t = 0.004\tau_0$. We also analyzed a trajectory of $N = 221\,184$ particles of GB$(3.0, 1.25, 2, 1)$, of length $1.7 \times 10^6$ steps with $\Delta t = 0.002\tau_0$, provided by the Bologna group [27].

Typical results are shown in Fig. 1. The splay and twist correlations are well fitted by an exponential form $c(k,t) = \exp(-\nu t)$, with the decay rate found to be accurately given by $\nu = \lambda k^2$, $\lambda$ being a constant. However, we see oscillatory decay of bend correlations in all the simulations,

$$c_{\text{bend}}(k,t) = \exp(-\nu t)\cos\omega t \ , \tag{1}$$

with $\nu = \lambda^{\text{r}} k^2$ and $\omega = \lambda^{\text{i}} k^2$. The $k^2$ behaviour of the decay rate $\nu$ and the frequency $\omega$ is illustrated in Fig. 2, and the fitted $\lambda$ coefficients are summarized in Table I.

To explain these results, we reprise the standard derivation of the coupled, time-dependent, differential equations in Fourier space for hydrodynamic flow and director reorientation [3, 12, 13]. These equations determine the relaxation in time of each Fourier component $\delta\tilde{\mathbf{n}}(\mathbf{k},t)$ and $\tilde{\mathbf{v}}(\mathbf{k},t)$ from an initial value towards equilibrium, at low $k$; by linear response theory, the same decay rates and oscillation frequencies will determine the forms of the corresponding equilibrium time correlation functions [1–3]. For twist and splay deformations, $k_1 = k$, $k_3 = 0$, and the velocity component $\tilde{v}_1 \equiv 0$ by the condition of incompressibility $\boldsymbol{\nabla} \cdot \mathbf{v} = 0$. Neglecting nonlinear inertial terms in the flow, and director inertia, as

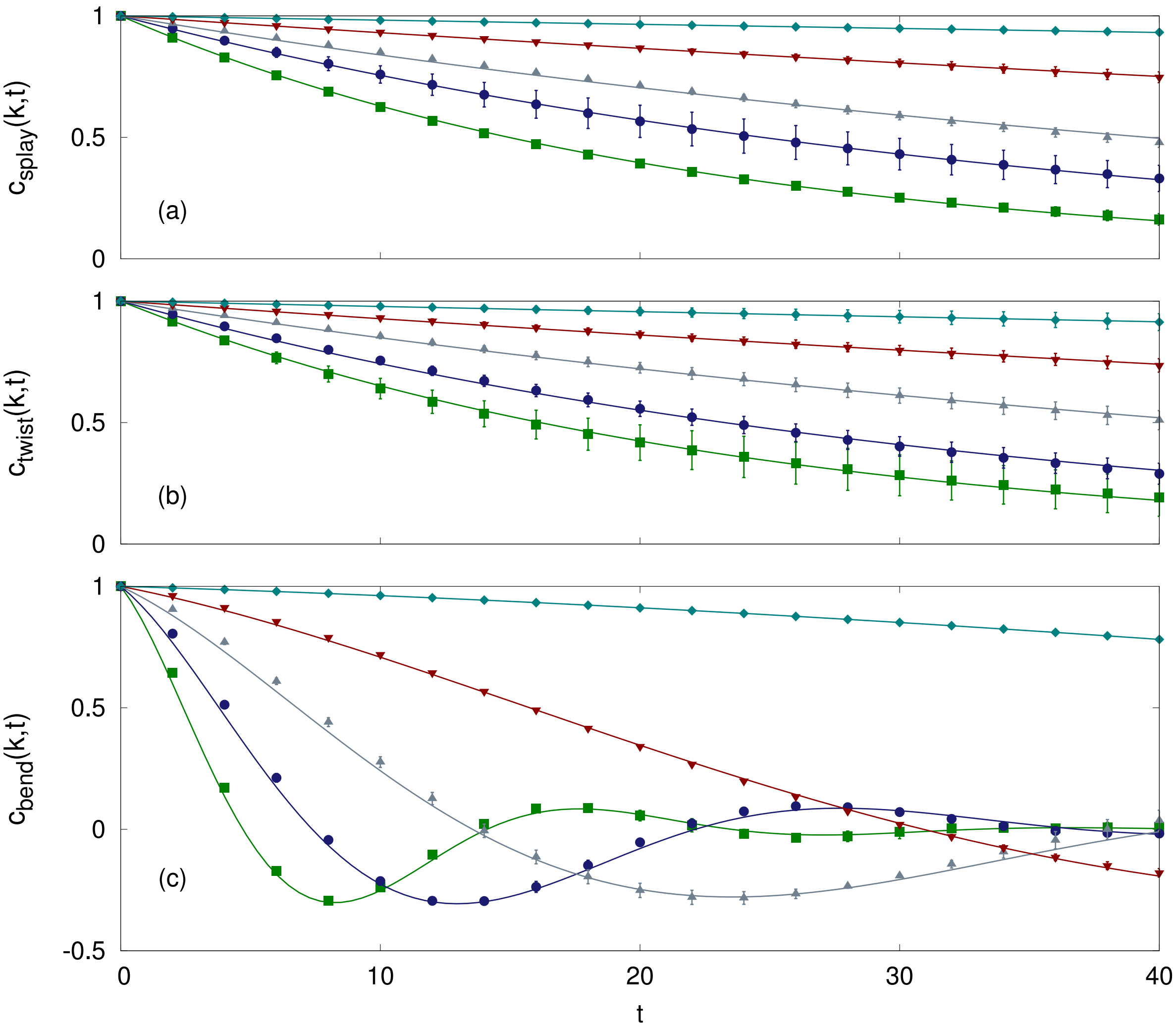

FIG. 1. Color online. Time correlation functions $c(k,t)$ plotted versus time $t$ for model GB$(3.0, 5.0, 1, 3)$ at $\rho = 0.3$, $T = 3.4$. (a) splay; (b) twist; (c) bend. Points with error bars are simulation results. Lines are the fits to an exponential decay, or to eqn (1), as discussed in the text. Different curves correspond to different wavenumbers $k = n2\pi/L$ where $L$ is the simulation box length: $n = 1$ (diamonds, cyan); $n = 2$ (down-triangles, red); $n = 3$ (up-triangles, grey); $n = 4$ (circles, blue); $n = 5$ (squares, green). All quantities are in simulation units defined in the text.

is usual, the relaxation equations for twist, involving the pair of variables $\{\delta\tilde{n}_2, \tilde{v}_2\}$ become

$$\big(\gamma_1\,\partial_t + K_2k^2\big)\delta\tilde{n}_2 = 0\ , \tag{2a}$$

$$\big(\rho\,\partial_t + \eta_3k^2\big)\tilde{v}_2 = 0\ , \tag{2b}$$

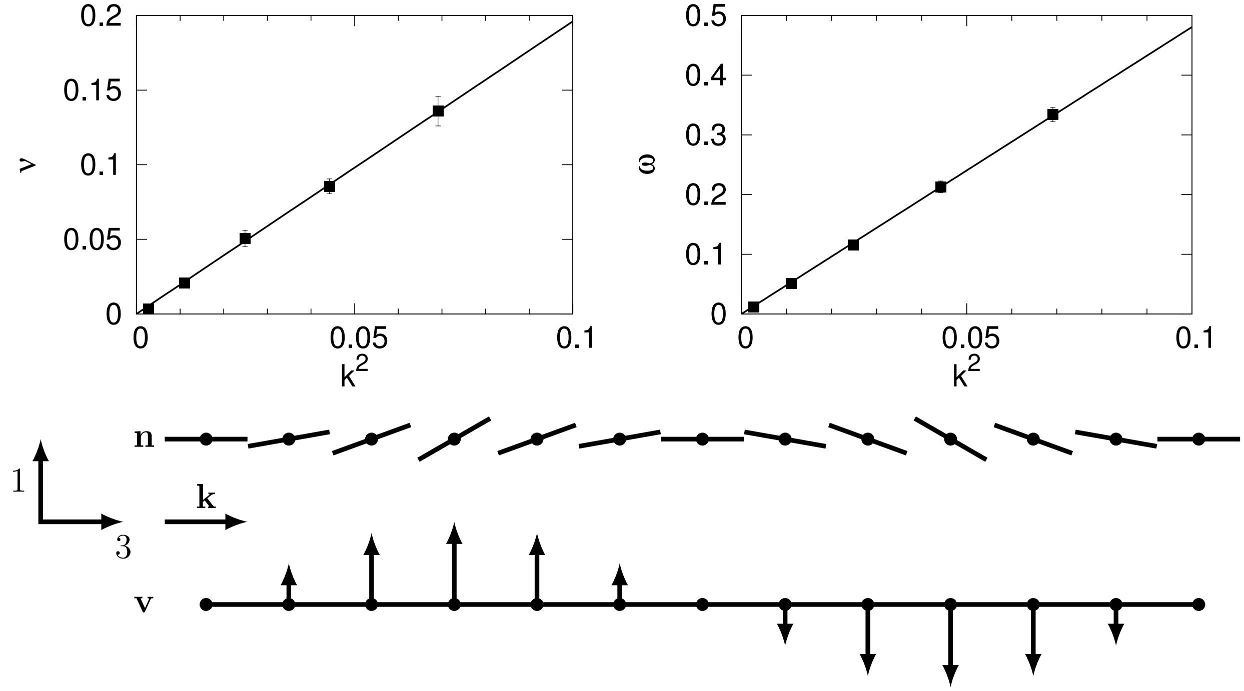

FIG. 2. Decay rates $\nu$ and oscillation frequencies $\omega$, obtained by fitting eqn (1) to $c_{\text{bend}}(k,t)$, as functions of $k^2$, for the same system as Fig. 1. Points with error bars are simulation results. Lines are linear least-squares fits. All quantities are in simulation units defined in the text. We also give a schematic illustration of the director variation **n** and coupled velocity field **v** for the bend mode.

where $\partial_t$ denotes the time derivative, and those for splay, in the variables $\{\delta\tilde{n}_1, \tilde{v}_3\}$, are

$$\big(\gamma_1\,\partial_t + K_1k^2\big)\delta\tilde{n}_1 + \mathrm{i}k\alpha_3\,\tilde{v}_3 = 0\ , \tag{3a}$$

$$-\mathrm{i}k\alpha_3\,\partial_t\,\delta\tilde{n}_1 + \big(\rho\,\partial_t + \eta_1k^2\big)\tilde{v}_3 = 0\ . \tag{3b}$$

$K_1$ and $K_2$ are respectively the splay and twist elastic constants, and $\rho$ is the mass density. The remaining quantities are determined by the Leslie coefficients $\alpha_i$: $\gamma_1 = \alpha_3 - \alpha_2$ is the rotational viscosity, while $\eta_1 = \frac{1}{2}(\alpha_3 + \alpha_4 + \alpha_6)$ and $\eta_3 = \frac{1}{2}\alpha_4$ are Miesowicz (shear) viscosities. In eqn (2) the director twist $\delta\tilde{n}_2$ and the transverse velocity $\tilde{v}_2$ are completely decoupled. The director relaxes according to $\delta\tilde{n}_2 \propto \exp(-\nu_{\text{twist}}t)$; the rate is given by $\nu_{\text{twist}} = \lambda_{\text{twist}}k^2 = K_2k^2/\eta_{\text{twist}}$, where the rotational (twist) viscosity $\eta_{\text{twist}} \equiv \gamma_1$. The velocity relaxes according to $\tilde{v} \propto \exp(-\nu'_{\text{twist}}t)$ with a rate $\nu'_{\text{twist}} = \lambda'_{\text{twist}}k^2 = \eta_3k^2/\rho$. Assuming that $\eta_3 \sim \eta_{\text{twist}} \sim 10^{-3}\,\text{Pa}\,\text{s} - 10^{-2}\,\text{Pa}\,\text{s}$, $K_2 \sim 10^{-11}\,\text{N}$, and $\rho \sim 10^3\,\text{kg}\,\text{m}^{-3}$, the two timescales

TABLE I. Elastic constants $K_1$, $K_2$, $K_3$, and time correlation function fit parameters $\lambda$, from MD simulations of three GB models at the indicated densities and temperatures. All quantities are in simulation units. Estimated errors in the last quoted digit are given in parentheses.

| $\rho$ | $T$ | $K_1$ | $K_2$ | $K_3$ | $\lambda_{\text{splay}}$ | $\lambda_{\text{twist}}$ | $\lambda^{\text{r}}_{\text{bend}}$ | $\lambda^{\text{i}}_{\text{bend}}$ |
|---|---|---|---|---|---|---|---|---|
| | | | | GB(3.0, 5.0, 2, 1) | | | | |
| 0.32 | 0.9 | 0.70(2) | 0.69(1) | 1.51(4) | 0.15(1) | 0.17(1) | 1.4(1) | 1.5(1) |
| 0.33 | 1.0 | 1.04(2) | 1.02(2) | 2.65(4) | 0.15(1) | 0.17(1) | 1.6(1) | 2.5(1) |
| 0.35 | 2.0 | 1.59(3) | 1.38(2) | 4.00(4) | 0.17(1) | 0.16(1) | 2.1(1) | 2.4(1) |
| 0.38 | 3.0 | 3.81(7) | 3.29(5) | 11.5(1) | 0.22(1) | 0.21(1) | 2.9(1) | 4.9(1) |
| | | | | GB(3.0, 5.0, 1, 3) | | | | |
| 0.3 | 3.4 | 3.17(3) | 2.84(2) | 6.01(4) | 0.66(1) | 0.64(1) | 1.96(2) | 4.81(3) |
| 0.3 | 3.45 | 2.88(2) | 2.52(2) | 4.95(3) | 0.70(1) | 0.70(1) | 2.11(6) | 4.08(6) |
| | | | | GB(3.0, 1.25, 2, 1) | | | | |
| 0.333 | 0.53 | 1.93(4) | 2.50(3) | 5.24(13) | 0.05(4) | 0.04(3) | 0.63(8) | 1.55(6) |

are well separated:

$$\frac{\nu_{\text{twist}}}{\nu'_{\text{twist}}} = \frac{\lambda_{\text{twist}}}{\lambda'_{\text{twist}}} = \frac{\rho K_2}{\eta_3 \eta_{\text{twist}}} \sim 10^{-4} - 10^{-2} \,.$$

For the splay mode, eqn (3), a secular equation for the decay rates is obtained by substituting $\partial_t \to -\nu = -\lambda k^2$:

$$\begin{vmatrix} -\nu\gamma_1 + K_1 k^2 & \mathrm{i}k\,\alpha_3 \\ \mathrm{i}k\,\nu\alpha_3 & -\nu\rho + \eta_1 k^2 \end{vmatrix} = 0$$

$$\Rightarrow \quad \lambda^2 \rho\gamma_1 + \lambda\big(\alpha_3^2 - \gamma_1\eta_1 - \rho K_1\big) + K_1\eta_1 = 0 \,. \tag{4}$$

If the timescale separation still applies, the two roots will be real, and will obey $\lambda \ll \lambda'$, in which case

$$\lambda'_{\text{splay}} \approx \frac{\eta_1 - \alpha_3^2/\gamma_1 + \rho K_1/\gamma_1}{\rho} \,,$$

$$\lambda_{\text{splay}} \approx \frac{K_1}{\gamma_1 - \alpha_3^2/\eta_1 + \rho K_1/\eta_1} \equiv \frac{K_1}{\eta_{\text{splay}}} \,,$$

where $\eta_{\text{splay}} = \gamma_1 - \alpha_3^2/\eta_1 + \rho K_1/\eta_1 \approx \gamma_1 - \alpha_3^2/\eta_1$. Director splay fluctuations are expected to be dominated by this slow mode $\lambda_{\text{splay}}$, relaxing exponentially at a rate $\nu_{\text{splay}} = \lambda_{\text{splay}} k^2 = K_1 k^2/\eta_{\text{splay}}$.

Our twist and splay results are almost indistinguishable from each other (see Table I); from them we may conclude that $\alpha_3$ is very small, that $\eta_{\text{splay}} \approx \eta_{\text{twist}} = \gamma_1$, and that $\rho K_1/\gamma_1^2 \approx \rho K_2/\gamma_1^2 \lesssim 10^{-2}$ for GB$(3.0, 5.0, 2, 1)$, and $\approx 5 \times 10^{-2}$ for GB$(3.0, 5.0, 1, 3)$, at the state points studied. These ratios are at the high end of the anticipated range, probably because coarse-grained rigid molecular models have lower viscosities and higher mobilities than more realistic ones. Nonetheless, they are still much less than 1, and all of this is in accord with the standard view.

For bend fluctuations, $k_1 = 0$, $k_3 = k$, and $\tilde{v}_3 \equiv 0$ by incompressibility. The coupled relaxation equations for the pair $\{\delta\tilde{n}_1, \tilde{v}_1\}$ (and similarly for $\{\delta\tilde{n}_2, \tilde{v}_2\}$) are

$$\big(\gamma_1\,\partial_t + K_3k^2\big)\delta\tilde{n}_1 + \mathrm{i}k\alpha_2\,\tilde{v}_1 = 0\ , \tag{5a}$$

$$-\mathrm{i}k\alpha_2\,\partial_t\,\delta\tilde{n}_1 + \big(\rho\,\partial_t + \eta_2k^2\big)\tilde{v}_1 = 0\ , \tag{5b}$$

where $\eta_2 = \frac{1}{2}(\alpha_4 + \alpha_5 - \alpha_2)$ is the remaining Miesowicz viscosity, and $K_3$ is the bend elastic constant. This mode is illustrated in Fig. 2. Substituting $\partial_t \to -\nu = -\lambda k^2$ gives the secular equation

$$\begin{vmatrix} -\nu\gamma_1 + K_3k^2 & \mathrm{i}k\,\alpha_2 \\ \mathrm{i}k\,\nu\alpha_2 & -\nu\rho + \eta_2k^2 \end{vmatrix} = 0$$

$$\Rightarrow\quad \lambda^2\rho\gamma_1 + \lambda\big(\alpha_2^2 - \gamma_1\eta_2 - \rho K_3\big) + K_3\eta_2 = 0\,. \tag{6}$$

A similar argument to the splay case would give well-separated real roots

$$\lambda'_{\text{bend}} \approx \frac{\eta_2 - \alpha_2^2/\gamma_1 + \rho K_3/\gamma_1}{\rho}\ ,$$

$$\lambda_{\text{bend}} \approx \frac{K_3}{\gamma_1 - \alpha_2^2/\eta_2 + \rho K_3/\eta_2} \equiv \frac{K_3}{\eta_{\text{bend}}}\ ,$$

where $\eta_{\text{bend}} = \gamma_1 - \alpha_2^2/\eta_2 + \rho K_3/\eta_2 \approx \gamma_1 - \alpha_2^2/\eta_2$. This leads to the usual prediction that bend relaxation is overdamped, occurring at a rate $\nu_{\text{bend}} = K_3k^2/\eta_{\text{bend}}$. However, our simulation results clearly do not conform to this: instead the oscillations correspond to complex roots

$$\lambda_{\text{bend}} = \lambda^{\text{r}}_{\text{bend}} + \mathrm{i}\lambda^{\text{i}}_{\text{bend}}\,.$$

To see how these arise, it is helpful to define two dimensionless quantities

$$\mu = \frac{\rho K_3}{\gamma_1\eta_2}\ , \qquad \alpha = 1 - \frac{\alpha_2^2}{\gamma_1\eta_2}\,.$$

We expect $\mu \sim 10^{-2}$ like the similar quantities defined above for twist and splay. Certainly, in both experiment [3, Table D.3], and simulation [28], typically $\eta_2 \gtrsim \gamma_1$, but also $K_3 \gtrsim K_2$, so $\mu = \rho K_3/\gamma_1\eta_2 \approx \rho K_2/\gamma_1^2$. The discriminant of the quadratic equation (6) gives complex roots if

$$(\alpha + \mu)^2 < 4\mu \quad \Rightarrow \quad |\alpha| \lesssim 2\sqrt{\mu} \ ,$$

assuming that $\mu \ll 1$. This is quite possible, depending on how close the viscosities $\gamma_1$, $\eta_2$, and $\alpha_2$ happen to be to each other. We already know that $\gamma_1 = \alpha_3 - \alpha_2 \approx |\alpha_2|$, since $\alpha_3$ is typically small, so if $\eta_2 \approx |\alpha_2|$, a small value of $\alpha$ will indeed result.

If $\mu \sim 10^{-4}$, then complex roots will only result if $|\alpha| < 0.02$; however, if $\mu \sim 10^{-2}$, complex roots will arise if $|\alpha| < 0.2$. To put this in context, Table D.3 of Ref. [3] gives typical experimental values of $\alpha = 0.18, 0.19, 0.23$ for MBBA near 25 °C, 5CB near 26 °C, and PAA near 122 °C, respectively. Wang *et al.* [29] have estimated the Leslie coefficients for the standard mixture E7, from which $\alpha = 0.06$ near 20 °C. Even smaller values come from theories, and from molecular simulation measurements of viscosities [28, 30–33]. The simulation results of Wu *et al.* [34], for the model GB(3.0, 5.0, 1, 2) [35], at $T = 2.5$, $\rho = 0.295$, give $\alpha \approx 0.01$. The theory of Kuzuu and Doi [36] for rodlike molecules predicts a value of $\alpha < 0.004$ over the entire nematic range. An affine transformation theory [37, 38] predicts values $\alpha < 0.1$ for molecules of elongation $\kappa \geq 3$ at modest nematic order parameters, and $\alpha \equiv 0$ in the perfectly aligned limit.

The parameter $\alpha$ appears in the continuum theory of switching phenomena, such as the homeotropic to planar-bend Freedericksz transition (see e.g. Chapter 5 of Ref. [3]). The influence of small values of $\alpha$ on backflow and kickback effects in such cases is well understood, but the generation of oscillatory director fluctuations in the bulk at low $k$ seems to have been overlooked. Our results show that these are easily observed in computer simulations of a range of coarse-grained molecular models. Moreover, they suggest that, even though overdamped decay is the norm in experiments, real-life examples might be found for which the secular equation (6) has complex roots, and the bend mode propagates. In this event, the roots are given by

$$\begin{aligned}
\lambda^{\mathrm{r}}_{\mathrm{bend}} &= (\alpha + \mu)\left(\frac{\eta_2}{2\rho}\right) \ , \\
\lambda^{\mathrm{i}}_{\mathrm{bend}} &= \sqrt{4\mu - (\alpha + \mu)^2}\left(\frac{\eta_2}{2\rho}\right) \ ,
\end{aligned}$$

both the prefactors being significantly smaller than 1. From the ratios $\lambda^{\mathrm{i}}_{\mathrm{bend}}/\lambda^{\mathrm{r}}_{\mathrm{bend}}$ measured in our simulations we can estimate $0.5 \lesssim \mu/(\mu+\alpha)^2 \lesssim 2$, which is completely consistent with $\alpha \sim \sqrt{\mu}$. The velocity field, of course, will be governed by the same dynamics as the director: there is no separation of timescales.

In conclusion, we have observed propagating director bend fluctuations in our simulations (and those of others) of different variants of the Gay-Berne nematic liquid crystal. We have shown that such modes are consistent with the equations of nematodynamics [7–11]. They may occur without violating the (traditionally assumed) condition $\mu = \rho K_3/\gamma_1\eta_2 \ll 1$. Values of $\mu \sim 10^{-2}$ may be sufficient to generate such modes, and seem to be quite typical in these Gay-Berne particle-based simulations. We may speculate that the relatively smooth nature of the Gay-Berne forces, compared with the full complexity of multiple atom-atom interactions, results in lower viscosities, and hence a value of $\mu$ near the high end of the expected range. The design of systems with low viscosities is one of the aims in liquid crystal device engineering, resulting in faster switching times, so these are prime candidates to observe the effect. The wider the “target window” determined by $\mu$, the more likely is the bend mode to propagate. The key requirement is that the dimensionless viscosity combination $\alpha = 1 - \alpha_2^2/\gamma_1\eta_2$ satisfies $\alpha \lesssim 2\sqrt{\mu}$. This may be attainable, even for the somewhat smaller values of $\mu$ typically seen in experiment, depending on the precise values of the viscosities $\alpha_2$, $\gamma_1$, and $\eta_2$. Therefore, it may not be out of the question to observe such propagating bend modes in real-life experimental systems. Taking these modes into account may be important for the accurate description of director field relaxation, and defect motion, in low-viscosity nematics. Similar conditions are unlikely to be satisfied for the splay modes, because the analogous key quantity is $1 - \alpha_3^2/\gamma_1\eta_1$, and the Leslie coefficient $\alpha_3$ is typically quite small compared with the others.

Computer facilities were provided by Warwick University Centre for Scientific Computing. Support from the Engineering and Physical Sciences Research Council is gratefully acknowledged. We are grateful to M. Ricci, R. Berardi, and C. Zannoni (Bologna) for providing the trajectory of the GB$(3.0, 1.25, 2, 1)$ system, and to G. Alexander (Warwick) for his comments on the manuscript. MPA acknowledges helpful conversations with participants at the Programme on the “Mathematics of Liquid Crystals” held at the Isaac Newton Institute for Mathematical Sciences in 2013.

---

[*] a.humpert@warwick.ac.uk

[†] m.p.allen@warwick.ac.uk

[1] P. G. de Gennes and J. Prost, *The Physics of Liquid Crystals*, second, paperback ed. (Clarendon Press, Oxford, 1995).

[2] S. Chandrasekhar, *Liquid Crystals*, 2nd ed. (Cambridge University Press, Cambridge, 1992).

[3] I. W. Stewart, *The Static and Dynamic Continuum Theory of Liquid Crystals: A Mathematical Introduction* (Taylor and Francis, 2004).

[4] C. Oseen, Trans. Faraday Soc. **29**, 883 (1933).

[5] H. Zocher, Trans. Faraday Soc. **29**, 945 (1933).

[6] F. C. Frank, Discuss. Faraday Soc. **25**, 19 (1958).

[7] J. L. Ericksen, Arch. Rational Mech. Anal. **4**, 231 (1960).

[8] F. Leslie, Arch. Rational Mech. Anal. **28**, 265 (1968).

[9] O. Parodi, J. de Physique **31**, 581 (1970).

[10] D. Forster, T. C. Lubensky, P. C. Martin, J. Swift, and P. S. Pershan, Phys. Rev. Lett. **26**, 1016 (1971).

[11] P. C. Martin, O. Parodi, and P. S. Pershan, Phys. Rev. A **6**, 2401 (1972).

[12] Orsay Liquid Crystal Group, J. Chem. Phys. **51**, 816 (1969).

[13] M. J. Stephen and J. P. Straley, Rev. Mod. Phys. **46**, 617 (1974).

[14] G. Durand, L. Leger, F. Rondelez, and M. Veyssie (Orsay Liquid Crystal Group), Phys. Rev. Lett. **22**, 1361 (1969).

[15] D. C. Van Eck and M. Perdeck, Mol. Cryst. Liq. Cryst. **49**, 39 (1978), http://dx.doi.org/10.1080/00268947808070325.

[16] R. Borsali, D. Y. Yoon, and R. Pecora, J. Phys. Chem. B **102**, 6337 (1998), http://dx.doi.org/10.1021/jp9813645.

[17] F. Giavazzi, S. Crotti, A. Speciale, F. Serra, G. Zanchetta, V. Trappe, M. Buscaglia, T. Bellini, and R. Cerbino, Soft Matter **10**, 3938 (2014).

[18] J. G. Gay and B. J. Berne, J. Chem. Phys. **74**, 3316 (1981).

[19] A. Humpert and M. P. Allen, “Elastic constants and dynamics in nematic liquid crystals,” In preparation.

[20] M. P. Allen and D. Frenkel, Phys. Rev. A **37**, 1813 (1988).

[21] M. P. Allen and D. Frenkel, Phys. Rev. A **42**, 3641 (1990), erratum.

[22] M. P. Allen, M. A. Warren, M. R. Wilson, A. Sauron, and W. Smith, J. Chem. Phys. **105**, 2850 (1996).

[23] R. Berardi, A. P. J. Emerson, and C. Zannoni, J. Chem. Soc. Faraday Trans. **89**, 4069 (1993).

[24] D. J. Cleaver, C. M. Care, M. P. Allen, and M. P. Neal, Phys. Rev. E **54**, 559 (1996).

[25] M. A. Bates and G. R. Luckhurst, J. Chem. Phys. **110**, 7087 (1999).

[26] E. de Miguel, Molec. Phys. **100**, 2449 (2002), http://dx.doi.org/10.1080/00268970210121605.

[27] D. Vanzo, M. Ricci, R. Berardi, and C. Zannoni, Soft Matter **8**, 11790 (2012).

[28] S. Sarman, J. Chem. Phys. **108**, 7909 (1998).

[29] H. Wang, T. X. Wu, S. Gauza, J. R. Wu, and S.-T. Wu, Liq. Cryst. **33**, 91 (2006), http://dx.doi.org/10.1080/02678290500446111.

[30] A. M. Smondyrev, G. B. Loriot, and R. A. Pelcovits, Phys. Rev. Lett. **75**, 2340 (1995).

[31] S. Cozzini, L. F. Rull, G. Ciccotti, and G. V. Paolini, Physica A **240**, 173 (1997).

[32] L. Bennett and S. Hess, Phys. Rev. E **60**, 5561 (1999).

[33] S. Sarman and A. Laaksonen, Chem. Phys. Lett. **479**, 47 (2009).

[34] C. Wu, T. Qian, and P. Zhang, Liq. Cryst. **34**, 1175 (2007), http://www.tandfonline.com/doi/pdf/10.1080/02678290701663878.

[35] G. R. Luckhurst, R. A. Stephens, and R. W. Phippen, Liq. Cryst. **8**, 451 (1990).

[36] N. Kuzuu and M. Doi, J. Phys. Soc. Japan **53**, 1031 (1984), http://dx.doi.org/10.1143/JPSJ.53.1031.

[37] H. Ehrentraut and S. Hess, Phys. Rev. E **51**, 2203 (1995).

[38] M. Kroger and S. Sellers, Mol. Cryst. Liq. Cryst. Sci. Technol. Sect. A **300**, 245 (1997), http://dx.doi.org/10.1080/10587259708042351.